Electrodeposition of Bi Thin Films on n-GaAs(111)B. Part II: Correlation between the Nucleation Process and the Structural and Electrical Properties.

Alicia Prados, Rocío Ranchal*

Department Física de Materiales, Universidad Complutense de Madrid, 28040, Madrid, Spain,

ABSTRACT

The surface morphology and the crystal structure of 40 nm thin Bi films electrodeposited on GaAs(111)B at different growth overpotentials have been studied by means of atomic force microscopy and X-ray diffraction, respectively. The Bi/GaAs interface has also been electrically characterized by means of current-voltage curves that have been analyzed with the Thermionic-Field Emission Theory. Taking into account the results presented in Part I, we can conclude that the structural and electrical properties of the Bi layers are correlated with the nucleation process and, therefore, with the energy band diagram of the semiconductor-electrolyte interface. We have found that surface morphology is directly dependent on the amount of protons adsorbed on the GaAs surface, whereas the crystal quality and the interfacial properties also depend on the nucleation mechanism (instantaneous or progressive).

Introduction

In Part 1 of this work, we present and analyze the current transients obtained during the nucleation of 40 nm thin Bi films electrodeposited onto n-GaAs(111)B at five different growth overpotentials (-0.15 V, -0.2 V, -0.3 V, -0.5 V and -0.7 V). As it is explained in Part I, to make clearer the presentation and discussion of the results it is useful to define the overpotential of the Semiconductor-electrolyte interface (SEI), η_{SEI}, as the bias applied to the n-GaAs/electrolyte junction i.e.,the difference between the applied potential, E, and the open circuit potential (OCP = 0.1 V vs. Ag/AgCl). Therefore, the η_{SEI} applied in this work is -0.25 V, -0.3 V, -0.4 V, -0.6 V and -0.8 V. Using the formalism developed by Palomar-Pardavé *et al.*[1], we have deconvoluted the current transients into their individual contributions, showing the concurrence of Bi(III) ion reduction together with the adsorption and reduction of protons (H^+). Thanks to this analysis we have observed a nonuniform dependence of these processes with η_{SEI} that can be explained on the basis of the nonuniform distribution of states in the energy band structure of the SEI. The competition of Bi(III) ion reduction with H^+ adsorption and reduction is complex because reduction reactions occur via energy bands, sometimes with the assistance of extrinsic surface states[2], whereas adsorption processes take place only via surface states[3,4]. Consequently, the correlation between the nucleation process and the overpotential is rather complex and is directly related to the energy band diagram of the SEI.

Once the processes involved in the nucleation are identified, it is possible to correctly interpret the influence η_{SEI} on the properties of the Bi film. In this work, we study the impact of η_{SEI} on the properties of 40 nm thick Bi films grown by dc electrodeposition. We have performed a structural and morphological analysis of the Bi layers, as well as the electrical characterization of the Bi/n-GaAs interface. Thanks to all these results, we can conclude that the morphological,

structural and electrical properties of the Bi film and the Bi/n-GaAs interface are clearly determined by the nucleation process through the competition between Bi(III) ion reduction and H^+ adsorption or reduction, which is controlled by the applied potential. We also report that the barrier height of the Schottky junction is strongly influenced by the presence of chemical species trapped at the interface. We would like to highlight that the deconvolution of the current transients recorded during the nucleation of the films present in Part I has been decisive for the correct interpretation of the measurements presented in this Part II.

Methods

The influence of η_{SEI} on the crystal structure and morphology of the Bi films has been determined by X-ray diffraction (XRD) and atomic force microscopy (AFM). Structural characterization was done by XRD using a Philips X'Pert PRO system equipped with a Cu target ($\lambda_{K\alpha}$ = 1.54 nm) and a four-circle goniometer. All films were measured in Bragg-Brentano configuration ($\theta - 2\theta$ scan) to determine the preferred orientation of the films. To avoid substrate reflections, an offset of 0.5° was introduced between the incidence and the diffracted direction ($\omega = \theta - \theta_{offset}$). In order to study the out-of-plane and in-plane crystal quality, ω-rocking curves and ϕ-scans have been performed, respectively. The average tilt and twist of Bi grains with respect the GaAs substrate is defined as one half of full width at half maximum (FWHM/2) of ω-rocking curves and ϕ-scans, respectively. In order to extract the FWHM values with their corresponding errors, the ω-rocking curves have been fitted to a pseudovoigt function and the φ-scans to a Gaussian function. The values obtained for the FWHM have been corroborated with the software X'Pert Data Viewer provided by PANalytical B. V. Surface characterization was done by means of a Nanoscope atomic force microscope with a Si tip, working in tapping mode and operating in air. Images were analyzed with WSxM 5.0 software and Nanoscope 5.31r1 software.

Finally, the Bi/GaAs interface was characterized electrically by means of current-voltage (*I-V*) curves. Several diodes with 230 and 250 μm diameter were fabricated in the Bi films by standard optical lithography followed by photochemical etching. Afterward, an electrical contact made by 15 nm Cr/150 nm Au was evaporated on the top of the Bi diodes to protect them. *I-V* measurements were carried out at 290 K in a Janis probe station (model CCR10-1) with a Hewlett Packard 4145 semiconductor parameter analyzer.

Results and Discussion

1. Morphological Characterization of Bi Layers

AFM images performed on the Bi films show a surface morphology in agreement with a 3D nucleation (Figure 1.a-e) as expected from the current-time transients presented in Part I of this work. This nucleation mechanism based on the formation and growth of 3D islands is common in the deposition of metals on semiconducting substrates due to the weak interaction between the adsorbed metal atoms and the semiconductor[5]. All films present small rounded islands that coalesce into more elongated features. As η_{SEI} increases a higher coalescence is observed as indicated by the decrease of the surface root mean square roughness (rms), the average height and the peak-to-peak values (Figure 1.f-g). Depth profiles taken from each AFM image (Figure 1.a-e) also reflect the progressive increase of film compactness as the η_{SEI} increases. At η_{SEI} = -0.6 V, the Bi film is still compact; however, the rms increases slightly and at η_{SEI} = -0.8 V there is a change of the surface morphology due to the appearance of round-shaped isolated islands. These isolated islands produce a large increase of the overall surface roughness, but the areas without isolated islands also present a slight increase of the rms.

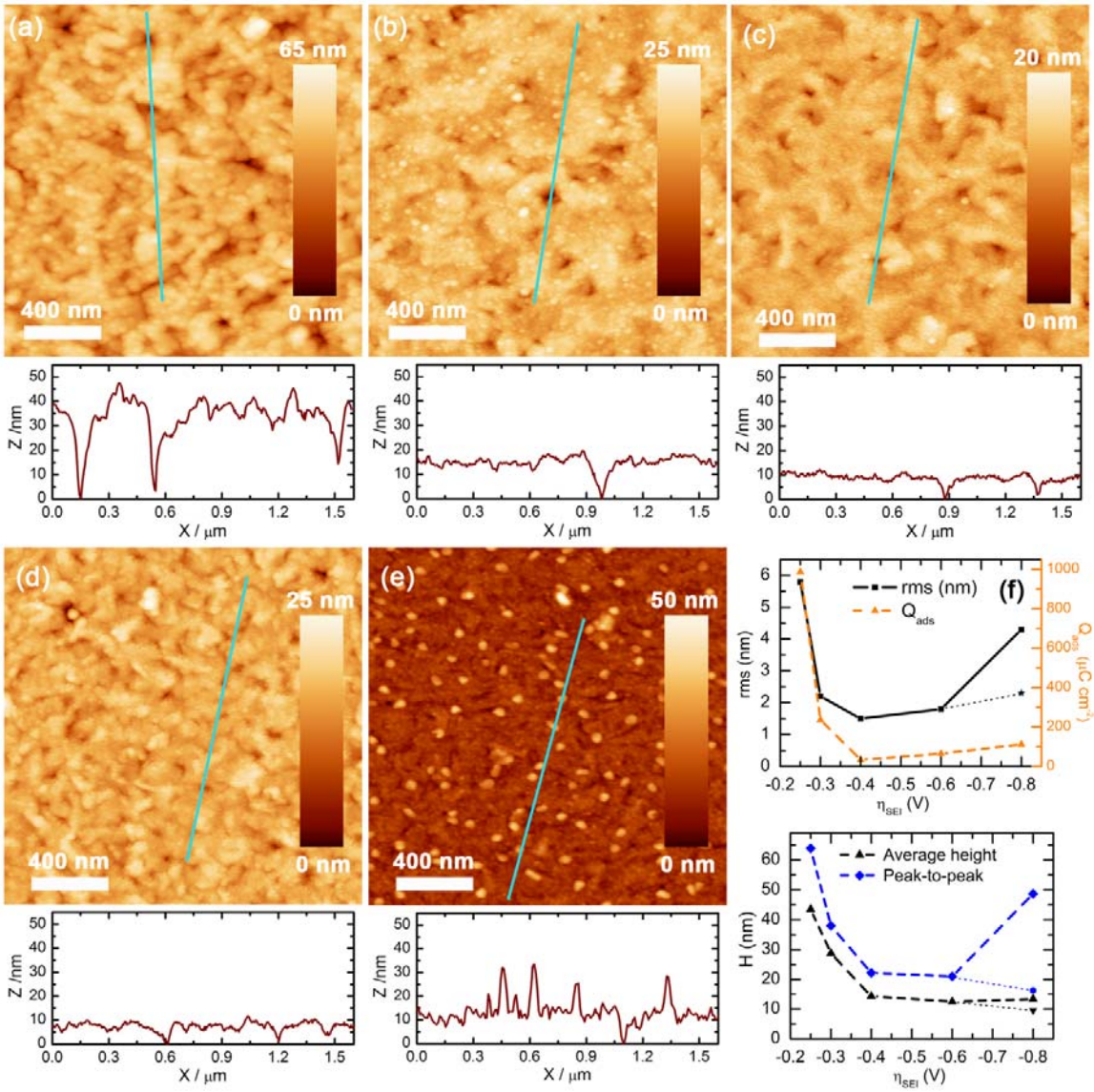

Figure 1. AFM images of 40 nm Bi layers grown on GaAs(111)B at η_{SEI} (a) -0.25 V, (b) -0.3 V, (c) -0.4 V, (d) -0.6 V and (e) -0.8 V. (f) Evolution of the surface roughness (rms) inferred from AFM images and Q_{ads} (Part 1) as a function of η_{SEI}. The point marked with ★ represents the rms of the areas without isolated islands. (g) Average height and peak-to-peak values obtained from AFM images as a function of η_{SEI}. The points marked with ▼ and ● represent the average height and the peak-to-peak value of the areas without isolated islands, respectively.

The evolution of surface morphology can be correlated with the evolution of the nucleation process (Part I), in particular with the behavior of H^+ adsorption (Figure 1.f). This adsorption process is characterized by a time constant, τ_{ads}, and the charge involved in the process, Q_{ads}[6]. As explained in Part I, H^+ adsorption seems to be a dynamic process and therefore, the amount of H_{ads} is only proportional to Q_{ads}. When Bi reduction follows a progressive or mixed nucleation due to a low nucleation rate (A), i.e., for η_{SEI} up to -0.4 V, the presence of H_{ads} that partially blocks the n-GaAs surface inhibits the formation of new Bi nuclei and hinders the development of the growing ones. Therefore, when the Q_{ads} is high, as at η_{SEI} = -0.25 V, the nucleation of the Bi film is considerably inhibited, and porous films with a high rms are obtained (Figure 1.a and f). As Q_{ads} diminishes, the Bi nucleation is enhanced, and flatter and more compact films are obtained (Figure 1.b–c and f). At η_{SEI} = -0.4 V, a considerable decrease of Q_{ads} is observed due to the enhancement of both the Bi(III) ions and H^+ reduction as a result of the assistance of surface states (Part I). This produces flat films with a low rms. However, in spite of the low Q_{ads} the Bi film still presents some imperfections that lead to a high peak-to-peak value (Figure 3.c). At η_{SEI} > -0.4 V the mechanism of Bi nucleation changes from progressive to instantaneous. Since all the Bi nuclei are formed at t = 0, the presence of H_{ads} and the concurrence of proton reduction do not have an influence on their formation but on the coalescence of the Bi nuclei. As the Q_{ads} increases, the coalescence is worse, and the rms increases (Figure 1.d–f). At η_{SEI} = -0.8 V the modification of the surface morphology coincides with the onset of the water reduction, and therefore, it could be related with a modification of the surface electronic structure induced by the adsorption of water molecules[4]. Taking into account these results, we can conclude that flatter Bi layers can be obtained when the amount of H_{ads} is reduced. This is in agreement with a recent study performed by the group of K. L.

Kavanagh[7] where it is observed that flatter Fe films with a better coalescence can be obtained by electrodeposition on n-GaAs substrates when the H_{ads} is reduced.

2. Structural Characterization of Bi Layers

XRD analysis has been carried out to check the effect of the growth potential on the Bi film crystallinity. A recent study showed that the growth procedure employed in this work (a CV followed by a dc electrodeposition) provides textured films assigned to the rhombohedral structure of metallic Bi ($R\bar{3}m$, 166) when deposited on GaAs substrates at -0.2 V[8]. Following that work, symmetric Bragg-Brentano XRD measurements have been carried out to determine the preferred orientation of the Bi layers grown at different η_{SEI} (Figure 2). In spite of the variation of the surface morphology with η_{SEI} (Figure 1.a-e), all the films exhibit a Bi(012) texture indicating the strong influence of the substrate surface orientation on the atomic arrangement of the Bi layer during the nucleation. Although the film grown at η_{SEI} =-0.8 V presents small contributions of Bi(003) and Bi(101) planes in its diffraction pattern, we can conclude that the crystal texture of the Bi layers is not influenced by the η_{SEI} but only by the substrate surface orientation, as we already reported[8]. In all cases, a small broad peak appears nearly at 36^{o} that could be attributed to surface oxidation. No peaks related to Bi-GaAs alloys are observed.

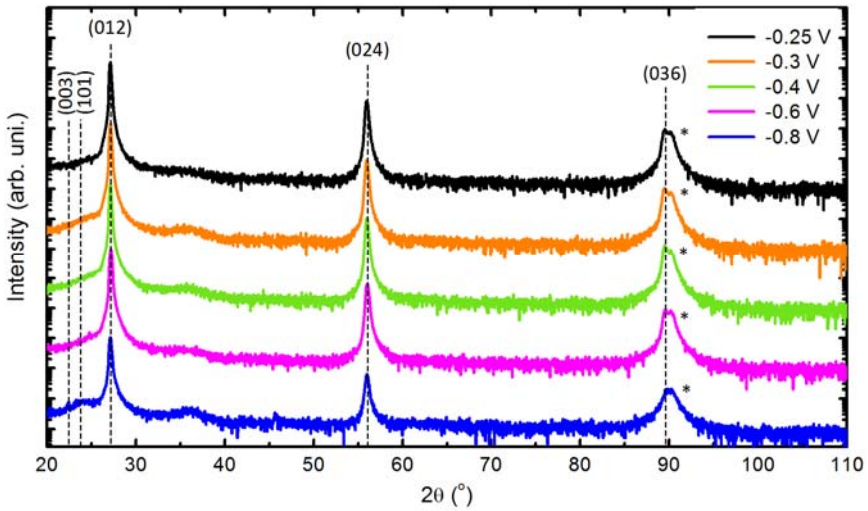

Figure 2. Bragg-Brentano XRD patterns of 40 nm-Bi films grown on GaAs(111)B substrates at different η_{SEI}. The dashed lines indicate the position of rhombohedral metallic Bi reflections (ICDD card 00-044-1246) that matches with an observed peak. Peaks marked with * correspond to the GaAs(333) reflection.

The out-of-plane crystallographic uniformity of the Bi films has been studied by means of ω-rocking scans performed around the Bi(024) Bragg reflection. It should be pointed out that the Bi(024) reflection has been used instead of the Bi(012) because the GaAs(111) reflection interferes with the latter whereas the GaAs(222) reflection does not interfere with the Bi(024). The ω-rocking curves show a decrease of the FWHM with η_{SEI} (Figure 3.a), indicating an enhancement of the out-of-plane crystallinity. The in-plane crystallographic uniformity of the Bi films has been analyzed by means of ϕ-scans (azimuthal scans) around the strongest asymmetric-Bragg reflections, i.e., reflections that are not related to the layer texture. In the case of Bi(012) films grown on GaAs(111)B, we have chosen the Bi(110) and GaAs(220) reflections (Figure 3.b). GaAs(220) shows three reflections in agreement with its 3-fold symmetry. Although Bi(110) has also a 3-fold symmetry, the azimuthal scan shows 12 reflections, which indicates that Bi grains are distributed in

four possible orientations with respect to GaAs(111)B planes[8]. The mosaicity of the Bi layers characterized by the averaged twist (FWHM/2) decreases with η_{SEI}, which indicates an enhancement of the in-plane crystallinity (Figure 3.a). On the contrary to surface morphology, the crystal quality of the Bi films only shows a constant improvement with η_{SEI}. We can conclude that the crystal quality is not apparently influenced by H^+ reduction but only by the presence of H_{ads} and the kinetics of Bi(III) reduction. At low η_{SEI} (from -0.25 V to -0.4 V), when Bi nucleation is progressive, the presence of H_{ads} inhibits the formation of new Bi nuclei and their correct match with the lattice of the GaAs surface. This initial bad atomic arrangement is maintained during the growth, and it is propagated through the whole film, leading to high values of FWHM of ω-rocking curves and φ-scans (Figure 3.a). As the Q_{ads} decreases with the η_{SEI} due to the enhancement of Bi (III) ions and H^+ reduction, the crystal quality of the film is improved and lower values of FWHM are obtained. At high η_{SEI} (-0.6 V and -0.8 V), the nucleation of the Bi film is instantaneous and therefore, the correct lattice match between Bi nuclei and the GaAs surface only depends on the kinetics of the reaction. This enhancement of the crystal quality with the η_{SEI} is in good agreement with the study performed by the group of K. L. Kavanagh[7] where it is observed that a better epitaxial growth of Fe on n-GaAs substrates is obtained when electrodepositing at higher current densities.

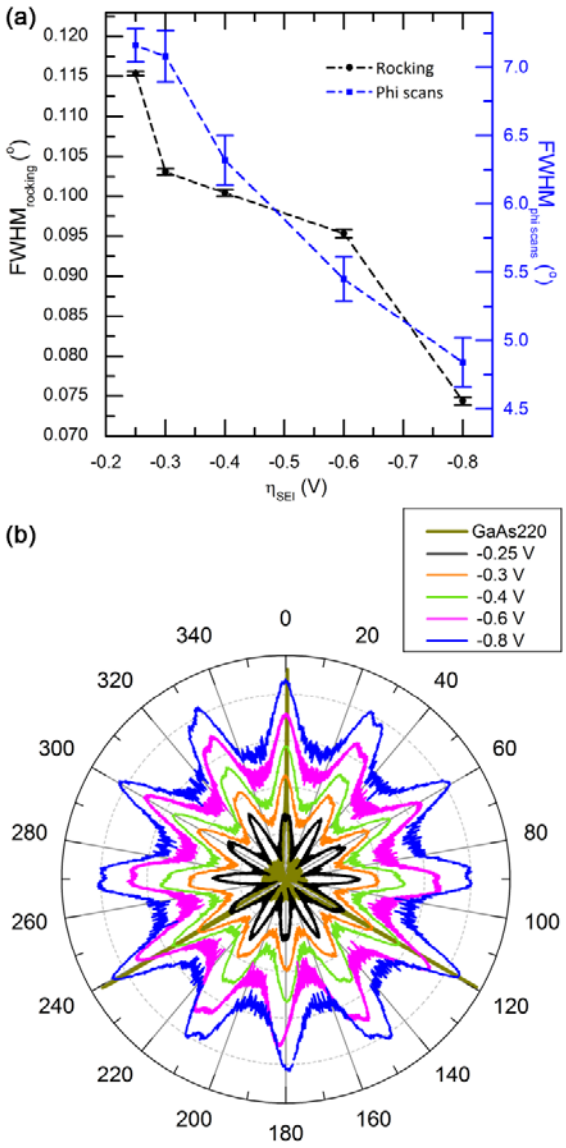

Figure 3. (a) FWHM of ω-rocking curves and φ-scans performed on the Bi films as a function of η_{SEI}. (b) Semilogarithmic polar diagrams of φ-scans performed on 40 nm-Bi thin films grown at different η_{SEI}.

3. Electrical Properties of Bi/n-GaAs Interfaces

The Bi/GaAs interface has been electrically characterized by means of *I-V* curves measured at 290 K on Bi/GaAs diodes of 230 and 250 μm diameter (Figure 4.a). All diodes showed a good reproducibility when measuring the *I-V* curves, making it possible to consider just one *I-V* curve per diode. In all cases, an excess current at the reverse bias has been observed that indicates tunnel transport through the Schottky barrier. This is a consequence of the high electron concentration of the GaAs substrates ($n \approx 1\cdot 10^{18}$ cm^{-3}) since GaAs Schottky diodes with $n > 1\cdot 10^{17}$ cm^{-3} exhibit sufficiently thin barriers at 290 K to allow electrons tunneling from the conduction band to the metal[9]. Consequently, I-V characteristics should be analyzed on the basis of Thermionic Field Emission (TFE) theory[10]. The analytical expression for the forward current in the TFE theory (j_{TFE}) derived by Padovani and Stratton for intermediate temperatures and intermediate-high biases[10] is given below:

$$j_{TFE} = j_S \cdot \exp\left(\frac{E}{E_0}\right) \tag{1}$$

where j_S is the saturation current; E_0 is an energy defined below; and E *is* the potential energy associated with the bias applied between the metal and the semiconductor that form the Schottky junction (V_D). To take into account the effect of the bulk of the semiconductor, the electrical contacts, and the probes used to perform the measurements, the whole system is modeled like a Schottky diode in series with a resistor of resistance R. Therefore, the potential energy applied to the Schottky junction is:

$$E = q \cdot V_D = q \cdot (V - I \cdot R) \tag{2}$$

where V is the applied bias and I is the current that flows through the system. The saturation current in eq. 1 is given by:

$$j_S = \frac{A^* T^2 \left[\pi \cdot E_{00} \cdot \left(q\phi_B - E + \xi\right)\right]^{\frac{1}{2}}}{k_B T \cdot \cosh\left(E_{00} \big/ k_B T\right)} \cdot \exp\left(\frac{\xi}{k_B T} - \frac{q\phi_B + \xi}{E_0}\right) \tag{3}$$

where A^* is the Richardson constant; T is the temperature; k_B is Boltzmann's constant; and ϕ_B is the barrier height. The Fermi energy measured with respect to the bottom of the conduction band ($\xi = E_F - E_C$) can be obtained by Nilsson approximation[11]:

$$\eta = \frac{E_F - E_C}{kT} = \frac{\ln u}{1 - u^2} + \frac{\left(\frac{3}{4}\sqrt{\pi} \cdot u\right)^{\frac{2}{3}}}{1 + \left[0.24 + 1.08 \cdot \left(\frac{3}{4}\sqrt{\pi} \cdot u\right)^{\frac{2}{3}}\right]^{-2}} \tag{4}$$

where E_F and E_C are the energy of the Fermi level and the edge of the conduction band, respectively. The parameter u is defined as:

$$u = F_{\frac{1}{2}}(\eta) = \frac{n}{N_C} \tag{5}$$

with n being the electron concentration and $N_C = 4.12 \cdot 10^{17}$ cm^{-3} the effective density of states for electrons in the conduction band of GaAs at 290 K[12]. Since $n > N_C$, the substrates are degenerate, and the concentration of electrons (described by Fermi-Dirac distribution) is approximately the concentration of ionized donors, being able to neglect hole population.

$$N_D^+ \approx n = N_C \cdot F_{\frac{1}{2}}(\eta) \tag{6}$$

The Richardson constant (A^*) can be expressed in terms of the Richardson constant for free electrons (A) and the tunneling mass (m_t) for the electrons[12]:

$$A^* = A \cdot \frac{m^*}{m_o} = A \cdot m_t = 120 \cdot 10^4 \cdot m_t \tag{7}$$

where m^* is the electron effective mass and m_o is the mass of free electrons. The energy E_0 is given by:

$$E_0 = E_{00} \cdot \coth\left(\frac{E_{00}}{k_B T}\right) \tag{8}$$

where

$$E_{00} = \frac{q \cdot h}{4\pi} \cdot \left(\frac{N_D^+}{m^* \cdot \varepsilon}\right)^{\frac{1}{2}} = \frac{q \cdot h}{4\pi} \cdot \left(\frac{N_D^+}{m_t \cdot m_o \cdot \varepsilon_d \cdot \varepsilon_0}\right)^{\frac{1}{2}} \tag{9}$$

Here h is Planck constant (in electronvolts); N_D^+ is the ionized donor concentration (equal to the electron concentration, n, in m^{-3}); ε_d is the semiconductor dynamic permittivity[13]; and ε_0 is the vacuum permittivity. It is mandatory to determine the value of n for each substrate because this parameter strongly affects the barrier height obtained from the fitting. To do so, *C-V* curves have been measured on Au/Cr/GaAs Schottky diodes fabricated on each sample. The electron concentration ($n = N_D^+$) was in agreement with the wafer specifications ($\sim 1 \cdot 10^{18}$ cm^{-3}) in all cases.

The experimental characteristics shown in Figure 4.a have been analyzed by a nonlinear fit of the experimental data to eq. 1 using the Marquardt–Levenberg algorithm, with ϕ_B and R as free parameters. The m_t has also been set as a free parameter because it can be affected by the crystal disorder at the interface[14]. The fitting has been limited to intermediate bias (from 0.07 V until 0.3 V) because eq. 1 is not adequate for low bias, and at high bias there are additional effects such as local heating that are not being considered and make the experimental curve differ from the theory[15]. Figure 4.b shows two experimental curves and their respective fittings. The best-fit parameters from at least 5 different diodes of two different diameters were weight averaged to give the values listed in Table 1. Parameter uncertainties have been considered as the standard deviation of the average since the errors given by the fitting were negligible (lower than 1%). To take into account the two different diode diameters, the average value of each parameter (ϕ_B, m_t and R) has been obtained for each diode diameter through the expression:

$$x^{(d_1)} = \frac{\sum_{i=1}^{b} x_i^{(d_1)}}{b} \tag{10}$$

with b being the number of diodes measured with a specific diameter d_1. The uncertainty of the averaged value has been considered as the standard deviation of the average[16]:

$$\Delta x^{(d_1)} = \frac{\sigma_x}{\sqrt{b}} = \sqrt{\frac{\sum_{i=1}^{b} (x_i^{(d_1)} - x^{(d_1)})^2}{b \cdot (b-1)}} \tag{11}$$

where σ_m is the standard deviation. Finally, the averaged values obtained for all diameters have been weight averaged to provide the final value of both the parameter and its uncertainty:

$$\left(\bar{x} + \Delta\bar{x}\right) = \frac{\sum_{i=1}^{w} \frac{x^{(d_i)}}{\left(\Delta x^{(d_i)}\right)^2}}{\sum_{i=1}^{w} \frac{1}{\left(\Delta x^{(d_i)}\right)^2}} \pm \frac{1}{\sqrt{\sum_{i=1}^{w} \frac{1}{\left(\Delta x^{(d_i)}\right)^2}}} \tag{12}$$

where w is the number of different diameters measured.

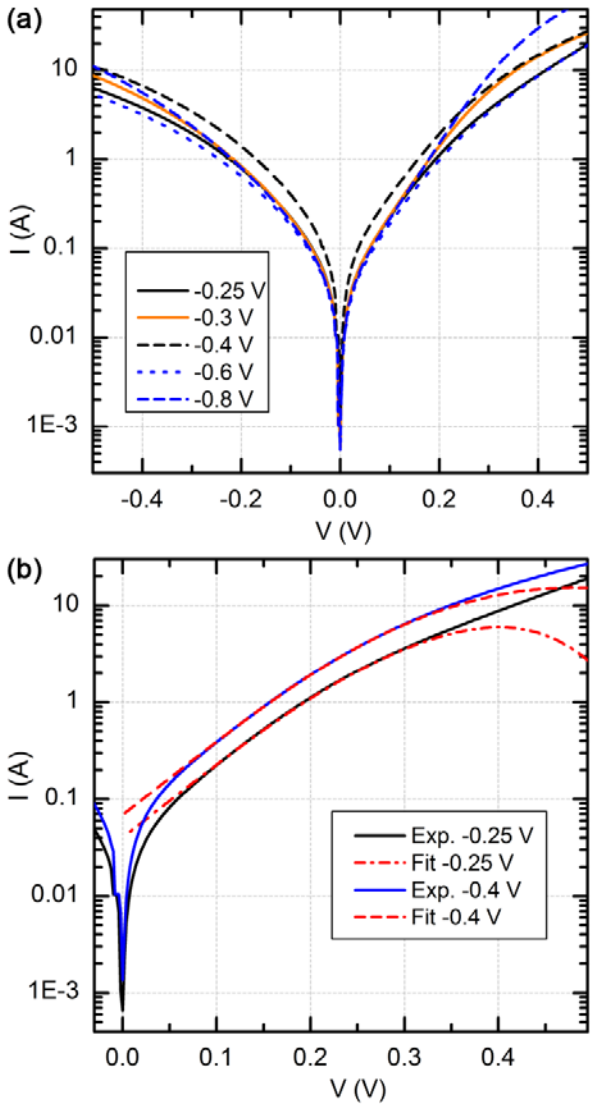

Figure 4. (a) *I-V* curves of Bi/GaAs diodes as a function of η_{SEI}. (b) Experimental characteristics measured on the samples grown at η_{SEI} = -0.25 V and -0.4 V and their respective fitting.

η_{SEI}(V)	ϕ_B (V)	$\Delta\phi_B$ (V)	m_t (10^{-3} m_o units)	Δm_t (10^{-3} m_o units)	R (Ω)	ΔR (Ω)
-0.25 V	0.8633	0.0039	10.51	0.17	25.60	0.66
-0.3 V	0.8260	0.0023	14.44	0.13	6.91	0.22
-0.4 V	0.8786	0.0038	15.17	0.32	7.28	0.64
-0.6 V	0.9125	0.0051	16.39	0.30	21.9	1.8
-0.8 V	0.82861	0.00037	18.499	0.066	2.604	0.078

Table 1. Average Values for Barrier Height (φ_B), Tunneling Mass (m_t), and Series Resistance (R) Derived from *I-V* Curves with their Respective Uncertainties.

The dependence of the tunneling mass, m_t, with η_{SEI} is shown in Figure 5.a. As expected, m_t is clearly related to the crystal order at the interface. The increase of m_t with η_{SEI} is related to the observed enhancement of the crystal quality also with η_{SEI} (Figure 3.a). Comparing the dependence of m_t, FWHM (ω-rocking) and FWHM (φ-scans) with η_{SEI}, we can conclude that m_t depends more strongly on the out-of-plane crystal quality (Figure 7.a).

The values obtained for ϕ_B are in agreement with those found in the literature for other n-GaAs Schottky barriers obtained by electrodeposition[17-20]. The dependence of ϕ_B with η_{SEI} is complex (Figure 5.b). In order to understand it, we have to take into account that our metal-semiconductor (M-S) junction cannot be considered as an intimate contact for several reasons: substrate roughness, adsorption of chemical species at the interface through dangling bonds, and surface defects[21, 22]. To take into account these effects, the M-S junction should be analyzed by means of the Bardeen model, which considers that the metal and the semiconductor are separated by a thin interfacial layer that contains interfacial states. As a consequence of this interfacial layer, the barrier height of the junction is described by:

$$q\phi_B = \gamma \cdot q(\phi_M - \chi) + (1-\gamma)\cdot(E_g - \phi_0) \tag{13}$$

where ϕ_M is the metal work function, χ is the semiconductor electron affinity, E_g is the semiconductor band gap, ϕ_0 is the neutral energy level for the interface states, and γ is a parameter that depends on the density of interface states, D_S [22]:

$$\gamma = \frac{1}{\left(1 + \frac{q \cdot D_S \cdot d}{\varepsilon}\right)} \tag{14}$$

where q is the electron charge, ε the semiconductor dielectric constant and d the thickness of the interfacial layer. These interfacial states are in fact Metal Induced Gap States (MIGS) or Virtual Induced Gap States (VIGS) which are a property of the semiconductor and are weakly dependent on the metal[2, 23]. These are intrinsic states of the semiconductor that have been perturbed by the metal due to the modifications induced on the matching conditions at the surface. Their neutral energy level, φ_0, must fall at or near the crossover branching point (E_B), which can be calculated from the 3D structure of the semiconductor[21, 22]. In the case of GaAs the theoretical value obtained for ϕ_0 is in the range of (0.5 – 0.55) eV, which has been experimentally confirmed by Cowley and Sze, who obtained ϕ_0 = 0.53 eV[23]. Due to the MIGS, an ideal Schottky junction can be considered in the Bardeen model as a junction with a high density of interfacial states. Therefore, the barrier height for an ideal n-GaAs Schottky junction is apparently independent of the metal work function (Mott-Schottky rule) and depends only on ϕ_0:

$$q\phi_B = E_g - \phi_0 \approx 0.92eV \tag{15}$$

This is approximately the value obtained in this work for the film grown at η_{SEI} = -0.6 V (Table 1). As we explained before, at η_{SEI} = -0.6 V the nucleation of Bi is instantaneous and consequently, the coupling between the Bi nuclei and the GaAs and, therefore, the interfacial properties depend only on the kinetics of Bi(III) ion reduction (Figure 5.a). For η_{SEI} = -0.8 V the

nucleation is also instantaneous but the barrier height decreases abruptly approximately to 0.1 eV, coinciding with the onset of water reduction (Table 1). Since the crystal quality of this layer is higher than the layer grown at η_{SEI} = -0.6 V (Figure 3.a), this decrease of the barrier height should be a consequence of a change of surface chemistry during the nucleation. A similar behavior was observed by De Vrieze *et al.*[20] with thick (75 and 150 nm) Au/n-GaAs Schottky barriers obtained by electrodeposition. In that work, the barrier height of the Schottky junctions decreases when they are electrodeposited at potentials more negative than the onset of water reduction. They ascribe this effect to the formation of metallic Ga due to cathodic decomposition of the GaAs. However, we have ruled out this possibility because GaAs is stable at our pH (pH = 0.1) and at this η_{SEI} (equivalent to a potential of E = -0.7 V vs. Ag/AgCl) according to its Pourbaix diagram[24]. Therefore, this decrease of the barrier height should be assigned to the onset of water reduction. This reaction leads to the formation of OH^- ions that can become adsorbed on the As atoms present on the surface, as has been observed by IR experiments[25], and remain adsorbed at the boundaries of the Bi islands. Due to the high electronegativity of the OH^- ions, the electrons of the As-OH bond will be transferred to the OH^- group, causing an excess of positive charge on the inside of the surface and an excess of negative charge on the outside of the surface[26]. This leads to a reinforcement of the original dipole of the GaAs surface according to the jellium model, which causes decrease of the effective Schottky barrier height.

For lower η_{SEI} (-0.3 V and -0.4 V), when the nucleation is progressive or mixed, the concurrent processes (H^+ adsorption and reduction) affect the lattice match between the Bi nuclei and the GaAs surface, and also the chemistry of the interface since some H^+ could get trapped at the island boundaries. The hydrogenation of the GaAs surface at the initial stages of the film growth can be considered as a passivation of the interfacial states (D_s decreases) because it inhibits the

formation of MIGS. According to the Bardeen model, when D_s decreases, $q\phi_B$ changes from $E_g - \phi_0$ = 0.92 eV (for metal/n-GaAs junctions[23]) to $q\cdot(\phi_m - \chi)$ = 0.36 eV (for Bi/GaAs junctions[12]), which is the expression corresponding to the Mott-Schottky rule. Consequently, as the η_{SEI} decreases and the surface hydrogenation is higher, ϕ_B decreases due to the passivation of the surface states, in agreement with other studies[27].

The film grown at η_{SEI} = -0.25 V presents an unexpected high ϕ_B taking into account the high adsorption of protons that takes place at this η_{SEI}. This could be explained on the basis of the high porosity of the film and taking into account that the films are exposed to air between their growth and the measurement of the *I-V* curves (Figure 3.a)[20, 28]. Consequently, when the metal of a Schottky junction is a porous film, the interface can become partially oxidized due to the air. This interfacial oxide layer could incorporate new interfacial states that can store additional charge at the interface. This would increase the barrier height according to the Bardeen model (eq. 13).

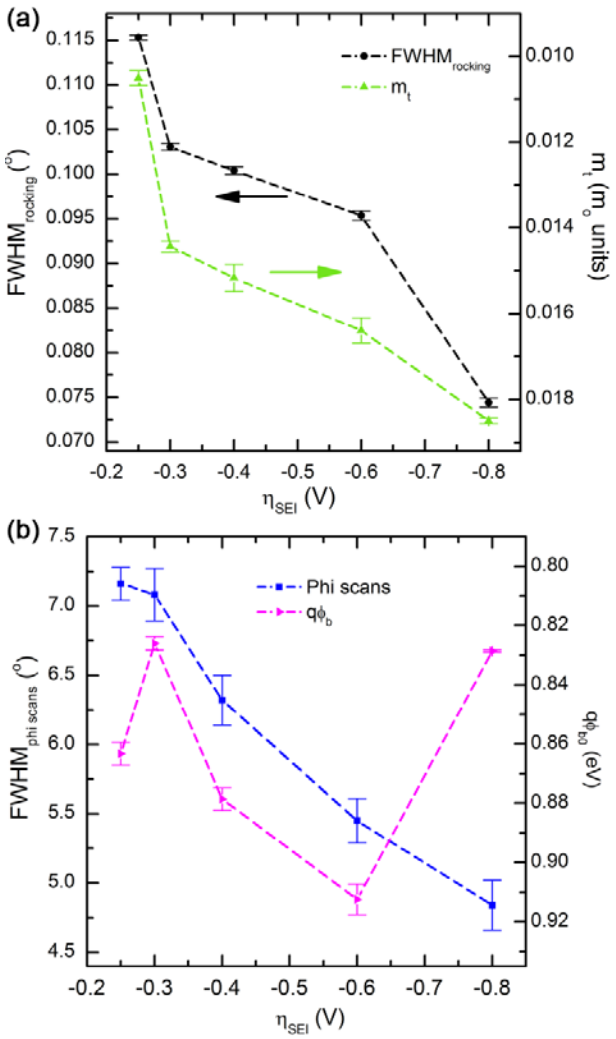

Figure 5. (a) Rocking curves FWHM and average tunneling mass (m_t) derived from *I-V* curves as a function of η_{SEI}. (b) Phi scans FWHM and average barrier height ($q \cdot \varphi_B$) derived from *I-V* curves as a function of η_{SEI}.

Conclusions

In this work we report the influence of η_{SEI} on the morphology, crystal structure and interfacial electrical properties of 40 nm-thick Bi layers electrodeposited on n-GaAs(111)B substrates. Experimental results indicate that the surface morphology and crystal quality are clearly correlated with the nucleation process (described in Part I of this work). At low η_{SEI} (-0.25 V), the presence of

H_{ads} inhibits both, the formation of new Bi nuclei and the coalescence of growing nuclei. This leads to films with poor crystal quality, a high roughness and a low compactness. As η_{SEI} increases (from -0.25 V to -0.4 V) and Bi reduction is enhanced, the amount of H_{ads} diminishes and the surface morphology and the crystal quality are enhanced. At high η_{SEI} (from -0.6 V to -0.8 V), the nucleation of the Bi film is instantaneous and, therefore, the lattice match between Bi grains and the GaAs surface is only dependent on the kinetics of the reaction. As the Bi(III) ion reduction reaction is enhanced, the crystal quality is improved. However, the increase of both proton adsorption and reduction inhibits the coalescence of Bi nuclei, increasing the roughness of the film. Finally, the electrical properties of the Bi/GaAs interface are dependent on both the crystal quality and the presence of chemical species trapped at the interface. The tunneling mass increases with η_{SEI} as the lattice match between the Bi layer and the GaAs surface is enhanced. The barrier height is also dependent on η_{SEI} through the structural quality of the interface, although it is strongly affected by the chemical composition at the interface. The presence of H_{ads} at the interface leads to lower values of the barrier height since it inhibits the formation of MIGS. The presence of OH^- groups also decreases the barrier height but because it enhances the original surface dipole of the GaAs. Finally, if the metal surface at the interface becomes oxidized, the barrier height can increase due to the formation of new interfacial states that can store additional charge. Taking into account all these results, we can conclude that the Bi layers with better properties are obtained when electrodeposited at a η_{SEI} in the range of -0.4 V to -0.6 V due to the combination of a low adsorption of protons and a high nucleation rate of Bi which leads to compact and flat layers, with a high quality lattice match with the n-GaAs substrate and a high Schottky barrier height. We would like to highlight the importance of the deconvolution of the current transients obtained during the nucleation of the Bi

films (Part I of this work) since it has allowed the correct interpretation of the dependence of the film and the interfacial properties with η_{SEI}.

AUTHOR INFORMATION

Corresponding Author

*a.prados@ucm.es

Phone: (+34) 91 394 4496; Fax: (+34) 91 394 4547

Author Contributions

The manuscript was written through contributions of all authors. All authors have given approval to the final version of the manuscript.

Acknowledgments

This work has been financially supported through project MAT2015-66888-C3-3-R of the Spanish Ministry of Economy and Competitiveness (MINECO/FEDER) and through the project PR26/16-3B-2 of Santander and Universidad Complutense de Madrid. We acknowledge the postdoctoral fellowship granted by Comunidad de Madrid and the European Union (PEJD-2016/IND-2233). We also acknowledge the use of facilities of Instituto de Sistemas Optoelectrónicos y Microelectrónica (ISOM).

References

* Part I of this work: Prados, A.; Ranchal, R. Electrodeposition of Bi Thin Films on n-GaAs(111)B. I. Correlation between the Overpotential and the Nucleation Process. *J. Phys. Chem. C* **2018**, 10.1021/acs.jpcc.8b01838.

1. Palomar-Pardavé, M.; Miranda-Hernández, M.; González, I.; Batina, N. Detailed Characterization of Potentiostatic Current Transients with 2D-2D and 2D-3D Nucleation Transitions. *Surf. Sci.* **1998**, *399*, 80-95. DOI: 10.1016/S0039-6028(97)00813-3

2. Memming, *R. Semiconductor Electrochemistry*; Wiley-VCH: Darmstadt, Germany, 2001. DOI: 10.1002/9783527613069.

3. Lüth, H. *Surface and Interfaces of Solid Materials*; Springer-Verlag Berlin Heidelberg: Berlin, Germany, 1995. DOI: 10.1007/978-3-662-03132-2.

4. Yoneyama, H.; Hoflund, G. B. Adsorption on Semiconductor Electrodes. *Prog. Surf. Sci.* **1986**, *21*, 5-92. DOI: 10.1016/0079-6816(86)90020-1

5. Oskam, G.; Long, J. G.; Natarajan, A.; Searson, P. C. Electrochemical Deposition of Metals on Silicon. *J. Phys. D: Appl. Phys.* **1998**, *31*, 1927-1949. DOI: 10.1088/0022-3727/31/16/001.

6. Hölzle, M. H.; Retter, U.; Kolb, D. M. The Kinetics of Structural Changes in Cu Adlayers on Au(111). *J. Electroanal. Chem.* **1994**, *371*, 101-109. DOI: 10.1016/0022-0728(93)03235-H.

7. Leistner, K.; Duschek, K.; Zehner, J.; Yang, M.; Petr, A.; Nielsch, K.; Kavanagh, K. L. Role of Hydrogen Evolution during Epitaxial Electrodeposition of Fe on GaAs. *J. Electrochem. Soc.* **2018**, *165*, H3076-H3079. DOI: 10.1149/2.0071804jes.

8. Prados, A.; Pérez, L.; Guzmán, A.; Ranchal, R. Mixed Effects of the Atomic Arrangement and Surface Chemistry on the Electrodeposition of Bi Thin Films on n-GaAs Substrates. *J. Phys. Chem. C* **2016**, *120*, 28295–28306. DOI: 10.1021/acs.jpcc.6b09144.

9. Rhoderick, E. H. Metal-Semiconductor Contacts. *IEE Proc. Part 1: Solid-State Electron Devices* **1982**, *129*, 1-14. DOI: 10.1049/ip-i-1.1982.0001.

10. Padovani, F. A.; Stratton, R. Field and Thermionic-Field Emission in Schottky Barriers. *Solid-State Electron.* **1966**, *9*, 695-707. DOI: 10.1016/0038-1101(66)90097-9.

11. Blakemore, J. S. Approximation for Fermi-Dirac Integrals, Especially the Function F1/2(η) Used to Describe Electron Density in a Semiconductor. *Solid State Electron.* **1982**, *25*, 1067-1076. DOI: 10.1016/0038-1101(82)90143-5.

12. Sze, S. M. *Physics of Semiconductor Devices.* John Wiley & Sons, Inc.: New York, USA, 1981.

13. Rideout, V. L.; Crowell, C. R. Effects of Image Force and Tunneling on Current Transport in Metal-Semiconductor (Schottky Barrier) Contacts. *Solid-State Electronics* **1970**, *13*, 993-1009. DOI: 10.1016/0038-1101(70)90097-3.

14. Kiziroglou, M. E.; Li, X.; Zhukov, A. A.; de Groot; P. A. J.; de Groot, C. H. Thermionic Field Emission at Electrodeposited Ni–Si Schottky Barriers. *Solid-State Electron.* **2008**, *52*, 1032-1038. DOI: 10.1016/j.sse.2008.03.002.

15. Stratton, R. Volt-Current Characteristics for Tunneling Through Insulating Films. *J. Phys. Chem. Solids* **1962**, *23*, 1177-1190. DOI: 10.1016/0022-3697(62)90165-8.

16. Taylor, J. R. *An Introduction to Error Analysis. The Study of Uncertainties in Physical Measurements*; University Science Books: Sausalito, California, USA, 1997.

17. Bao, Z. L.; Kavanagh, K. L. Epitaxial Bi/GaAs Diodes Via Electrodeposition. *J. Vac. Sci. Technol. B* **2006**, *24*, 2138-2143. DOI: 10.1116/1.2218874.

18. Vereecken, P. M.; Searson, P. C. Electrochemical Deposition of Bi on GaAs (100). *J. Electrochem. Soc.* **2001**, *148*, C733-C739. DOI: 10.1149/1.1406493.

19. Reineke, R.; Memming, R. High Barrier GaAs/Metal Schottky Junctions Produced by Electrochemical Metal Deposition. *Surf. Sci.* **1987**, *192*, 66-80. DOI: 10.1016/S0039-6028(87)81162-7.

20. De Vrieze, A.; Strubbe, K.; Gomes, W. P.; Forment, S.; Van Meirhaeghe, R. L. Electrochemical Formation and Properties of n-GaAs/Au and n-GaAs/Ag Schottky Barriers: Influence of Surface Composition Upon the Barrier Height. *Phys. Chem. Chem. Phys.* **2001**, *3*, 5297-5303. DOI: 10.1039/b104887m

21. Mönch, W. *Electronic Structure of Metal-Semiconductor Contacts.* Springer: Netherlands, 1990. DOI: 10.1007/978-94-009-0657-0.

22. Rhoderick, E. H.;Williams, R. H. *Metal-semiconductor contacts.* Oxford University Press: Oxford, UK, 1988.

23. Cowley, A. M.; Sze, S. M. Surface States and Barrier Height of Metal Semiconductor Systems. *J. Appl. Phys.* **1965**, *36*, 3212-3220. DOI: 10.1063/1.1702952.

24. Li, J.; Peter, L. M. Surface Recombination at Semiconductor Electordes.: Part IV. Steady-State and Intensity Modulated Photocurrents at n-GaAs Electrodes. *J. Electroanal. Chem.* **1986**, *199*, 1-26. DOI: 10.1016/0022-0728(86)87038-3.

25. Erné, B. H., Ozanam, F. y Chazalviel, J. -N. The Mechanism of Hydrogen Gas Evolution on GaAs Cathodes Elucidated by In Situ Infrared Spectroscopy. *J. Phys. Chem. B* **1999**, *103*, 2948-2962. DOI: 10.1021/jp984765t.

26. Leung, T. C.; Kao, C. L.; Su, W. S.; Feng, Y. J.; Chan, C. T. Relationship between surface dipole, work function and charge transfer: Some exceptions to an established rule. *Phys. Rev. B: Condens. Matter Mater. Phys.* **2003**, *68,* 195408. DOI: 10.1103/PhysRevB.68.195408.

27. Forment, S.; Biber, M.; Van Meirhaeghe, R. L.; Leroy, W. P.; Türüt, A. Influence of hydrogen treatment and annealing processes upon the Schottky barrier height of Au/n-GaAs and Ti/n-GaAs diodes. *Semicond. Sci. Technol.* **2004**, *19*, 1391–1396. DOI: 10.1088/0268-1242/19/12/011.

28. Vereecken, P. M.; Vanalme, G. M.; Van Meirhaeghe, R. L.; Cardon, F.; Gomes, W. P. Electrochemical reduction vs. vapour deposition for n-GaAs/Cu Schottky-barrier formation: A comparative study. *J. Chem. Soc., Faraday Trans.* **1996**, *92*, 4069-4075. DOI: 10.1039/FT9969204069

TOC Graphic